Neutron reflectometry studies of Gd/Nb and $Cu_{30}Ni_{70}$/Nb superlattices

Y Khaydukov[1,2,3], E Kravtsov[4,5], R Morari[6,7], D Lenk[7], L Mustafa[1,8], G Kim[1], M Trapp[9], V Zhaketov[10], V Proglyado[4], V Zrdavkov[6,7], Y Nikitenko[10], H-A Krug von Nidda[7], T Keller[1,2], R Steitz[9], R Tideks[7], A Sidorenko[6], V Ustinov[4,5], V Aksenov[10] and B Keimer[1]

[1]Max-Planck-Institut für Festkörperforschung, Stuttgart, Germany
[2]Max Planck Society Outstation at MLZ, Garching, Germany
[3]Skobeltsyn Institute of Nuclear Physics, Moscow State University, Moscow, Russia
[4]Institute of Metal Physics, Ural Branch, Russian Academy of Sciences, Ekaterinburg, Russia
[5]Ural Federal University, Ekaterinburg, Russia
[6]D. Ghitsu Institute of Electronic Engineering and Nanotechnologies ASM, Kishinev, Moldova
[7]Institut für Physik, Universität Augsburg, Augsburg, Germany
[8]Centre for Innovation Competence SiLi-nano, Martin-Luther-University Halle-Wittenberg, Halle, Germany
[9]Helmholtz-Zentrum für Materialien und Energie, Berlin, Germany
[10]Joint Institute for Nuclear Research, Dubna, Russia

E-mail: y.khaydukov@fkf.mpg.de

Abstract. We performed a comparative study of magnetic proximity effects in $[Gd(5nm)/Nb(25nm)]_{12}$ and $[Cu_{30}Ni_{70}(6nm)/Nb(27nm)]_{12}$ superlattices of S/F type by means of transport measurements and neutron scattering. Transport measurements have shown that Gd/Nb and CuNi/Nb superlattices shows 3D and 2D type of superconductivity respectively. In the case of proximity coupled Gd/Nb superconductor the effective thickness of the superconducting region, 300nm is enough to expel significant amount of applied magnetic field which was detected by neutron scattering. In decoupled CuNi/Nb superlattice thickness of every superconducting layer is only 27nm which is not enough to expel applied magnetic field. Our study shows how neutron reflectometry can be applied to study proximity coupling in superconducting/ferromagnet heterostructures.

1. Introduction

Artificial superconducting/ferromagnet (S/F) heterostructures are attracting nowadays great attention due to rich proximity effect physics arising in them [1-8]. In addition to scientific interest to the rich physics in S/F heterostructures there is also a growing interest to the application of these structures in superconducting spintronics [9-11] including such new approaches as neuromorphic computing [12,13]. At the moment most efforts are focused on simple S/F structures while usage of more complex S/F systems, such as $[S/F]_n$ (n>>1) superlattices (SL) may bring essentially new properties.

One may expect appearance of such properties for the SLs with thickness of the S and/or F layer becomes comparable with the coherence length of superconductivity in the S (ξ_S) or F (ξ_F) layers [14-16]. Preparation of such SLs requires, as in case of simple S/F structures, proper choice of materials with thin but magnetic and superconducting F and S layers, transparent S/F interface and many others. In addition, the manufacture of a periodic structure imposes additional conditions on the repeatability of the S/F interface through the whole structure. One potential candidate for S/F systems is a Gd/Nb heterostructure. Advantage of gadolinium is that it is a weak ferromagnet with Curie temperature only $T_F = 293$K which in combination with Nb, the strongest elemental superconductor with bulk T_C =9.3K, allows for preparation of S/F systems with comparable ferromagnetic and superconducting energies. Moreover gadolinium is able to couple with other ferromagnets [18-20] forming non-trivial magnetic ordering patterns which can be used for the creation of superconducting spin-valves. Our study of Nb(25nm)/Gd(d_F)/Nb(25nm) trilayers has shown that structures with highly transparent S/F interfaces and rather high correlation length $\xi_F = 4$nm can be grown [17]. Based on this study we prepared $[\mathrm{Gd}(d_F)/\mathrm{Nb}(25\mathrm{nm})]_{12}$ SLs with $d_F \sim \xi_F$ and studied them using Polarized Neutron Reflectometry (PNR) [21]. In the PNR experiment we measured spin-up $R^+(Q)$ and spin-down $R^-(Q)$ reflectivities as a function of momentum transfer Q. Analysis of the neutron spin asymmetry $S(Q) \equiv (R^+ - R^-)/(R^+ + R^-)$ allowed us to restore the depth profile of in-plane magnetization above and below T_C. In particular below T_C we have observed a suppression of neutron spin asymmetry which we attributed to a partial suppression of ferromagnetic order of Gd layers. This magnetic proximity effect is explained by screening of the applied magnetic field by proximity coupled Nb layers. This investigation showed that electromagnetic effects may have a considerable influence on magnetic properties of S/F systems [22].

Another ferromagnet widely used in study of proximity effects is Cu_xNi_{1-x} alloy [23-29]. The advantage of Cu_xNi_{1-x} is possibility to control the exchange energy by varying concentration of copper and nickel. So, for the well-studied $Cu_{40}Ni_{60}$ alloy the Curie temperature is only $T_m \sim 120$K, which leads to a quite high $\xi_F \sim 10$nm. For this study we used somewhat stronger $Cu_{30}Ni_{70}$ alloy with $T_m = 295$K [27], i.e. close to the Curie temperature of bulk Gd. Using an expression $\xi_F \sim T_m^{-1/2}$ we can estimate ξ_F for $Cu_{30}Ni_{70}$ alloy as $\xi_F \sim 6$nm, of the same order as ξ_F for Gd. Aim of this work is comparison of the magnetic proximity effect in Gd/Nb and CuNi/Nb SLs having similar structural and magnetic properties.

2. Experimental

For the study we chose two as similar as possible structures with $d_F \sim \xi_F$ and thick Nb layers with $d_S >> \xi_S$. The $[\mathrm{Gd}(5\mathrm{nm})/\mathrm{Nb}(25\mathrm{nm})]_{12}$ SL used in this study was prepared at ULVAC MPS-4000-C6 magnetron sputtering system in the Institute of Metal Physics (Ekaterinburg, Russia) according to the recipe described in details in our prior works [17,19]. The $[\mathrm{Cu}_{30}\mathrm{Ni}_{70}(6\mathrm{nm})/\mathrm{Nb}(27\mathrm{nm})]_{20}$ sample was prepared by a UNIVEX magnetron sputtering device in Augsburg University (Augsburg, Germany) [27]. Structural characterization of the layers and interfaces quality was performed using X-ray and neutron reflectometry. One needs, however, to note that due to a negligible optical contrast of CuNi and Nb materials [26] the X-ray reflectometry is ineffective for studying CuNi/Nb SLs. Neutron studies of Gd/Nb SLs were performed at the time-of-flight reflectometer REMUR (Dubna, Russia) and angle dispersive reflectometer NREX (Garching, Germany). The CuNi/Nb SLs were measured at angle dispersive reflectometer V6 (Berlin, Germany) and NREX. Figure 1 shows neutron reflectivities taken at room temperature with non-polarized beam. Curves are featured with total reflection plateau at $Q < Q_{crit}$ and well-pronounced Bragg peaks positioned at $Q_m \approx 2\pi m/D$ ($D = d_F+d_S$) arising from the diffraction on a superlattice [30]. Presence of big number ($m \geq 3$) of Bragg peaks speaks about high repeatability of S/F bilayer. One can also notice a smeared total reflection plateau and supressed intensity of the Bragg peaks for Gd/Nb SL comparing to CuNi/Nb system. There feature is explained by a high neutron absorption of ^{155}Gd and ^{157}Gd isotopes present in Gd layers [31-33].

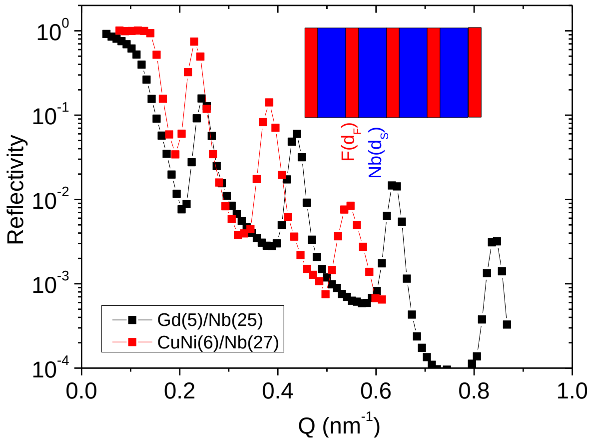

Figure 1. Neutron reflectivities taken at room temperature on the $[Gd(5)/Nb(25)]_{12}$ and $[CuNi(6)/Nb(27)]_{20}$ samples. Inset shows a sketch of the structure where blue and red colors indicate Nb and Gd or CuNi layers.

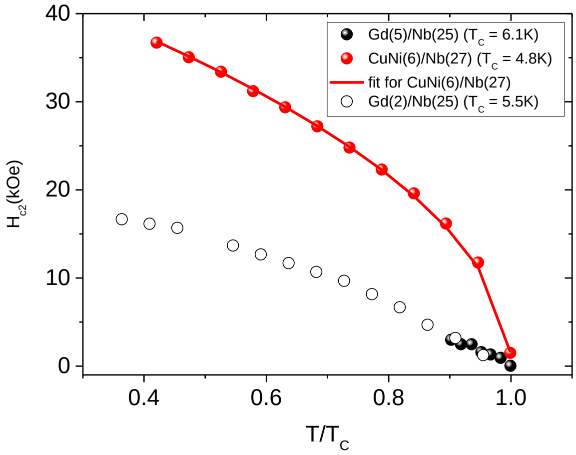

Figure 2. Temperature dependencies of the upper critical field measured on the same samples.

Superconducting properties of the samples were determined using standard four point electrical resistivity measurement with magnetic field applied in-plane. Figure 2 shows the temperature dependence of the upper critical field $H_{C2}(T)$. The dependence for the CuNi/Nb sample has a typical for 2D superconductivity square-root dependence $H_{C2}(T) = H_{C2}(0)(1\text{-}T/T_C)^{1/2}$ with $H_{C2}(0) \approx 6\ \Phi_0/(2\pi\xi_S\, d_S)$. We were able to fit this dependence for fixed d_S = 27nm with ξ_S = 5.2nm and T_C = 4.8K. The obtained correlation length can be compared with $\xi_S \approx$ 6nm reported previously for $Cu_{40}Ni_{60}$/Nb systems [24,25]. The Gd/Nb SL, in contrast, has linear $H_{C2}(T)$ dependence at least in the vicinity of T_C = 6.1K which evidences 3D superconductivity in the sample. Due to the limit of magnetic field H_{max}=5kOe at this setup we were not able to measure $H_{C2}(T)$ for higher fields. However, the $H_{C2}(T)$ dependence measured before [21] for $[Gd(2nm)/Nb(25nm)]_{12}$ superlattice showed linear dependence in a wider range of temperatures (see open circles in figure 2).

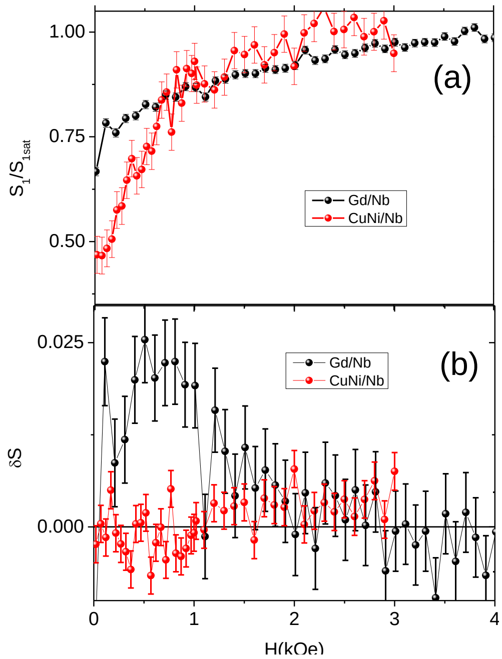

Figure 3. (a) Saturation-normalized spin asymmetry of the first Bragg peak measured above T_C. (b) Difference of spin asymmetries above and below T_C for the same samples.

Thus transport measurements reveal significant difference in superconducting properties of CuNi/Nb and Gd/Nb samples. In order to check this finding we performed low-temperature PNR experiments. Figure 3a shows the field dependence of the spin asymmetry at first Bragg peak, S_1, measured at $T = 1.1T_C$ for Gd/Nb and $T = 1.3T_C$ for CuNi/Nb SLs. For both samples the $S_1(H)$ dependence grows from remanence to saturation at fields of 1-2kOe. Figure 3b shows the difference of spin asymmetries $\delta S(H) \equiv S_1(T>Tc) - S_1(T<Tc)$ above and below T_C. For the measurements in superconducting state we used $T = 0.5T_C$ for Gd/Nb and $T = 0.2T_C$ for CuNi/Nb samples. For the Gd/Nb sample we observed statistically significant δS speaking about presence of magnetic proximity effect while for CuNi/Nb sample such a difference was not observed.

3. Discussions and conclusion

Thus transport measurements show that despite of similar thickness of F layer the Gd/Nb and CuNi/Nb SLs are of different type of superconductivity: the Gd/Nb is 3D and CuNi/Nb is 2D superconductor. By means of PNR we proved this observation. Indeed, Gd/Nb being a coupled superconductor with total thickness exceeding several times magnetic screening length $\lambda_{Nb} \sim 100$nm is able to screen partially applied magnetic field below T_C and supress magnetic response of F layers. The CuNi/Nb sample, in turn, is a set of not coupled Nb(27nm) layers so that magnetic field easily penetrates inside them and magnetic proximity effect is not observed. The absence of magnetic proximity effect in CuNi/Nb sample can be explained by a small interface transparency for superconducting correlations. This small transparency may be explained by a peculiarity of the deposition machine [27]. In this machine a substrate travels between CuNi and Nb sources in different chambers. Time of traveling, around 1 min for one CuNi/Nb bilayer, may be enough for a partial oxidation of Nb surface leading thus to a degradation of interface transparency. Another reason, though less plausible, is $\xi_F << d_F$ which will decouple S layers. In order to get real values of ξ_F and interface transparency one may analyze $T_C(d_F)$ dependency which will be done elsewhere.

In conclusion we performed a comparative study of magnetic proximity effects in Gd/Nb and CuNi/Nb superlattices of S/F type by means of transport measurements and neutron scattering. Transport measurements have shown that Gd/Nb (CuNi/Nb) SLs behaves like a 3D (2D) superconductor. In the case of proximity coupled Gd/Nb superconductor the effective thickness of the superconducting region is enough to expel significant amount of applied magnetic field to be detected by PNR. Opposite, when the S layers are decoupled in CuNi/Nb superlattice, effective thickness of superconductors is less than magnetic screening length and hence no strong flux expel is detected by PNR.

Acknowledgments

The authors would like to thank H. Kolb and P. Bieber for their assistance with low-temperature part of the measurements at NREX. We would like to thank HZB for the allocation of neutron time at V6 and financial support during experiment there. Stuttgart and Augsburg teams acknowledge support by Deutsche Forschungsgemeinschaft (DFG, German Research Foundation) – Project No. 107745057 – TRR 80. Research in Ekaterinburg was performed within the state assignment of Minobrnauki of Russia (theme "Spin" No. AAAA-A18-118020290104-2) and was partly supported by RFBR (Project No. 19-02-00674). RM and AS would like to acknowledge "SPINTECH" project of the HORIZON-2020 TWINNING program (2018-2020).

References

[1] Izyumov Yu A, Proshin Yu N and Khusainov M G 2002 *Phys. Usp.* **45** 109
[2] Golubov A A, Kupriyanov M Y and Il'ichev E 2004 *Rev. Mod. Phys.* **76** 411
[3] Buzdin A I 2005 *Rev. Mod. Phys.* **77** 935
[4] Eschrig M 2011 *Phys. Today* **64** 43
[5] Sidorenko A 2017 *Low Temp. Phys.* **43** 766
[6] Satapathy D K *et al* 2012 *Phys. Rev. Lett.* **108** 197201

[7] Das S *et al* 2014 *Phys. Rev.* B **89** 094511
[8] Mineev V P 2017 *Phys. Usp.* **60** 121
[9] Golubov A A and Kupriyanov M Y 2017 *Nat. Mater.* **16** 156
[10] Lenk D *et al* 2017 *Phys. Rev.* B **96**, 184521
[11] Zdravkov V I *et al* 2013 *Appl. Phys. Lett.* **103** 062604
[12] Schneider M L, Donnelly C A and Russek S E 2018 *J. Appl. Phys.* **124** 161102
[13] Soloviev I I, Schegolev A E, Klenov N V, Bakurskiy S V, Kupriyanov M Y, Tereshonok M V, Shadrin A V, Stolyarov V S and Golubov A A 2018 *J. Appl. Phys.* **124** 152113
[14] Klenov N *et al* 2019 *J. Nanotechnol.* **10** 833
[15] Bakurskiy S V, Kupriyanov M Y, Baranov A A, Golubov A A, Klenov N V and Soloviev I I 2015 *JETP Lett.* **102** 586
[16] Nevirkovets I and Mukhanov O A 2018 *Supercond. Sci. Technol.* **31** 03LT01
[17] Khaydukov Yu N *et al* 2018 *Phys. Rev.* B **97** 144511
[18] Drovosekov A B, Savitsky A O, Kholin D I, Kreines N M, Proglyado V V, Makarova M V, Kravtsov E A and Ustinov V V 2019, *J. Magn. Magn. Mater.* **475** 668
[19] Antropov N O, Khaydukov Yu N, Kravtsov E A, Makarova M V, Progliado V V and Ustinov V V 2019 *JETP Lett.* **109** 406
[20] Antropov N O, Kravtsov E A, Khaidukov Yu N, Ryabukhina M V, Proglyado V V, Weschke O and Ustinov V V 2018 *JETP Lett.* **108** 341
[21] Khaydukov Yu N, Kravtsov E A, Zhaketov V D, Progliado V V, Kim G, Nikitenko Yu V, Keller T, Ustinov V V, Aksenov V L and Keimer B 2019 *Phys. Rev.* B **99** 140503(R)
[22] Mironov S, Mel'nikov A and Buzdin A 2018 *Appl. Phys. Lett.* **113** 022601
[23] Nagy B *et al* 2013 *J. Supercond. Nov. Magn.* **26** 1957
[24] Zdravkov V, Sidorenko A, Obermeier G, Gsell S, Schreck M, Müller C, Horn S, Tidecks R and Tagirov L R 2006 *Phys. Rev. Lett.* **97** 057004
[25] Zdravkov V I *et al* 2010 *Phys. Rev.* B **82** 054517
[26] Khaydukov Yu, Morari R, Soltwedel O, Keller T, Christiani G, Logvenov G, Kupriyanov M, Sidorenko A and Keimer B 2015 *J. Appl. Phys.* **118** 213905
[27] Khaydukov Yu *et al* 2017 *J. Phys.: Conf. Ser.* **862** 012013
[28] Zhaketov V D, Nikitenko Yu V, Petrenko A V, Vdovichev S N, Churakov A V and Csik A 2018 *J. Exp. Theor. Phys.* **127** 508
[29] Feng Li, Wei Peng and Zhen Wang 2019 *Chinese Phys. Lett.* **36** 047401
[30] Pay attention that the position of the Bragg peaks in the vicinity to critical edge are distorted from the Bragg law due to the refraction effect. See e.g. Appendix B in [17]
[31] Frank A I, Bodnarchuk V I, Geltenbort P, Karpikhin I L, Kulin G V and Kulina O V 2003 *Physics of Atomic Nuclei* **66** 1831
[32] Nikova E S, Salamatov Y A, Kravtsov E A and Ustinov V V 2017 *Superlattices Microstruct.* **109** 201
[33] Khaydukov Yu, Kravtsov E, Progliado V, Ustinov V, Nikitenko Yu, Keller T, Aksenov V and Keimer B 2016 *J. Phys.: Conf. Ser.* **746** 012064